Chapter 10

CHEMICAL DOSIMETERS DEVELOPMENT AT IPEN FOR THE RADIATION PROCESSES QUALITY CONTROL

Ana Maria Sisti Galante[*] and Letícia Lucente Campos

Instituto de Pesquisas Energéticas e Nucleares, IPEN – CNEN/SP

Abstract

Different chemical compounds have been studied aiming to optimize dosimetric systems in radiation processes. The absorbed dose measurement that induces beneficial changes in the irradiated material characteristics is the most efficient method to monitoring the radiation process quality. The chemical dosimetry is a dosimetric method very useful in high doses measurements. Chemical changes radiation induced in liquid, solid or gaseous can be measured and quantified by means of espectrophotomety, termoluminescence or electronic paramagnetic resonance techniques and then the absorbed dose can be determined. A variety of chemical dosimeters is available however, same time these materials are not adequate for monitoring all types of products and irradiation conditions. The necessity of developing high quality dosimeters whose cost is viable to the irradiation installations to assure the quality of their processes, have stimulated the researchers to study new compounds that can be used in the irradiations routine control. When the used dosimeter and the studied species have approximately the same density and atomic composition the dosimetry is facilitated; the chemical dosimeters offer these conditions. Aiming to improve the dosimetry processes used in Brazil the High Doses Laboratory - HDL of the Instituto de Pesquisas Energéticas e Nucleares – IPEN/CEN-SP developed and studied four different chemical dosimeters: bromocresol green solutions, potassium nitrate (KNO_3) pellets pure and mixed with manganese dioxide (MnO_2), Fricke gel dosimeter (FXG) and dyed polimethylmethacrylate radiochromic films. The optical absorption (OA) measures were chosen to study the dosimetric properties and evaluate the advantages and disadvantages of each dosimeter. The main dosimetric properties studied were: incident radiation energy and angle dependence, ambient conditions influence and dose rate response; stability before and after irradiation; reproducibility and response accuracy. The preparation method, the cost of raw materials and use easiness were evaluated. The obtained results shown that the addition of MnO_2 in the KNO_3 pellets extend the dose range of KNO_3 dosimeter from between 1 and 150 kGy to 150

---

[*] E-mail address: sgalante@ipen.br;

and 600 kGy. PMMA films produced using dye Macrolex® red 5B can be applied to measure dose range between 5 and 100 kGy, bromocresol green solution doses from 1 to 15 kGy and Fricke gel dosimeter (FXG) presents useful dose a range between 5 and 50 Gy. These four dosimeters are of easy obtaining, low cost and simple use and can be applied to ^{60}Co monitoring in industrial irradiation processes routine dosimetry.

Introduction

The XIX century marks the beginning of the atomic physics development and two discoveries contributed so that this occurred: in 1895, the German physicist Wilhelm Konrad Röentgen discovers a radiation of unknown nature calling it of radiation X or X-rays. One year later, the French physicist Antonie Henry Becquerel intensifies its studies with the uranium mineral and discovers radioactive emissions that can penetrate in the matter. The Polish physicist Marie Sklodowska Curie intrigued with Becquerel's discovery fractionated the uranium mineral and isolated two new elements, the radium and the polonium. The knowledge of the radioactive decay was not work of only one person, but it is contribution resulted of many studious [1].

Soon after the discoveries of X-rays and radioactivity it was observed that radiation could cause changes in matter and damage to health. The radiation chemical effect depends on the matter composition and the amount of deposited energy by the radiation.

Radiation processing is a rapidly growing industry involving the improvement of several materials by ionizing radiation: electron beam; X-rays; gamma radiation [2, 3].

Several dosimetric materials such as alanine [4,5], LiF [6-8], radiochromic films [9,10] and organic dyed polymer[11] are examples of solid dosimeters; ceric-cerous solution, ferrous - ceric solution, ferrous sulphate solution (Fricke dosimeter) [12,13] are liquid dosimeters and nitrogen oxide and carbon dioxide [14-16] are examples of gaseous dosimeters, among others, and different techniques thermoluminescence [17], spectrophotometry [18,19], electronic paramagnetic resonance [20,21], magnetic resonance image [22-24] has been studied and applied to optimize the quality control used in radiation processing.

The High Doses Laboratory - HDL of the Instituto de Pesquisas Energéticas e Nucleares – IPEN/CNEN-SP develops materials to be applied in high doses dosimetry. The purpose of this research is to obtain materials of simple preparation method, low cost of raw materials and use easiness that can improve the quality control of radiation process. In the last years different materials such as potassium nitrate (KNO_3) pellets pure and mixed with manganese dioxide (MnO_2), bromocresol green solutions, Fricke gel dosimeter (FXG) and dyed polimethylmethacrylate radiochromic films were developed and characterized to be applied as dosimetric material. Results on gamma radiation decomposition of mixtures that contain KNO_3 and compounds such as $Ba(NO_3)_2$, KBr and MnO_2, a new radiation-sensitive indicator in aqueous solution form, the development and characterization of a new PMMA detector produced in Brazil and a Fricke gel dosimeter performance are reported. The studied parameters were: absorption spectrum and signal stability of irradiated and non-irradiated detectors; batch reproducibility; effect of the environmental conditions, dose-response useful range and dose rate dependence response [25-28].

Radiation Dosimetry

The dosimeters are classified as primary, reference, transfer and routine according to their intrinsic accuracy and application. Primary standards enable an absolute measurement of absorbed dose and are held by national standards laboratories; there are two types – ionizing chambers and calorimeters. A reference dosimeter is defined as a dosimeter of high metrological quality that can be used as a reference standard to calibrate other dosimeters; examples of dosimeters include chemical dosimeters, such as the Fricke, ceric-cerous, dichromate solutions and alanine dosimeters. A transfer dosimeter is used for transferring dose information from an accredited or national laboratory to an irradiation facility in order to establish traceability to that standards laboratory; example alanine, Fricke and dichromate solutions. A routine dosimeter is a dosimeter whose performance is often not as good as that of a reference dosimeter, but whose cost and ease of use make it suitable for day-to-day measurements in a radiation processing facility; examples of commonly used routine dosimeters are systems based on polymethylmethacrylate (PMMA), both dyed and un-dyed, cellulose tri-acetate and thin radiochromic films. The ideal dosimeter must possess adequate reproducibility and stability before and after irradiation, independence response on dose rate, on radiation incidence angle and incident radiation energy, environmental conditions stability and simple preparation and analysis [29].

Chemical Dosimetry

In chemical dosimetry the radiation dose is determined from quantitative chemical changes in the irradiated medium that can be solid, gaseous and liquid [30-33].

Solid systems: The solid state materials consist normally of organic or inorganic crystalline compounds (amino acids [4, 5], lithium fluoride [6-8]), amorphous or almost crystalline (ceramics [6, 34], glasses [35-37], plastics dyed [11] and semiconductors [38, 39]). In routine activities it is more interesting to use the solid dosimeters, because they present adequate dimensions and mechanical resistance to the hard works in industrial radiation processing. The measurement techniques used are spectrophotometry, thermoluminescence, electron spin resonance and lyoluminescence.

Dosimetric systems based on radiolytic decomposition of inorganic nitrates are used in quality control programmes of radiation processing. The final products formed are NO_2^- and O_2 that can be related with the dose. The radiation induced effect of added inorganic compounds on nitrates pellets has been studied. When a sample is exposed to ionising radiation the energy is absorbed by all the components present in the system such as cation, anions and the added substances. The enhancement/retardation in the decomposition of nitrates by various additives has been explained in terms of their electron donor/acceptor properties [40-48].

Polymethylmethacrylate (PMMA) dosimetry systems are commonly applied in industrial radiation processing [49]. The PMMA detector provides a means of directly estimating the absorbed dose. Under the influence of ionizing radiation chemical reactions take place in the material, creating and/or enhancing absorption bands in the visible and/or ultraviolet regions of the spectrum. The absorbed dose is determined by using an experimental calibration curve obtained by irradiating of a set of detectors with known absorbed doses aiming the quality
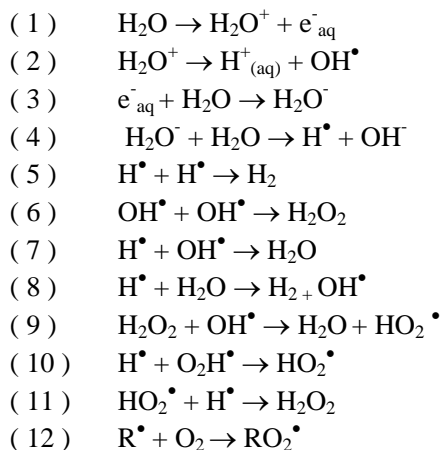
control of the radiation process and presenting excellent results. Dyed PMMA detectors produced at the High Doses Laboratory of IPEN using yellow, green, blue and red coloring compounds were previously characterized based on ^{60}Co gamma response. Their responses were compared with red 4034 Perspex and gammachrome YR detectors commercially available using the optical absorption (OA) technique [27, 28].

Gaseous systems: The gaseous systems have been applied for the quality control of irradiations of gases. Radiolysis of a gas may generate ions, excited atoms and molecules and free radicals. Many experimental techniques have been employed to study gas-phase reaction mechanisms, including permanent product analysis, measurements of ion currents, mass spectrometry, pulse radiolysis, the effects of scavengers, and isotopic labeling. The frequent types of reactions include direct formation of electronically excited molecules [14-16].

Liquids systems: When an ionizing radiation, i.e., gamma radiation or high-energy electrons, passes through a liquid medium, water, organic solvent or a combined mixture of water and organic solvent, ionizations and excitations occur along the trajectory. Aqueous solutions are the most used dosimeters to evaluate the absorbed dose. The dosimetric system is based on the reactions of solutes with the species formed in the radiolysis of water, as example can be cited – ferrous sulphate dosimeter (Fricke dosimeter); ferrous-cupric sulphate dosimeter; ceric sulphate (or ceric-cerous sulphate dosimeter; dichromate dosimeter; ethanol-chlorobenzene dosimeter and radiochromic dye solutions [33].
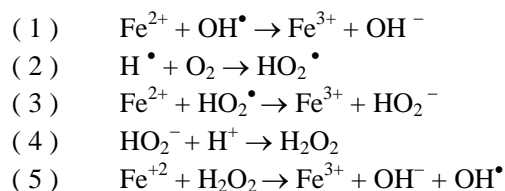
The radiation-chemical reactions with the water, produces free radicals and molecular products. Hydrogen atoms (H), hydroxyl radicals (OH) and hydrated electrons (e^-_{aq}) constitute the free radicals group; hydrogen (H_2) and hydrogen peroxide (H_2O_2) constitute the molecular products group [32].

The chemical species formed in an aqueous solution are the following:

$$(1) \quad H_2O \rightarrow H_2O^+ + e^-_{aq}$$
$$(2) \quad H_2O^+ \rightarrow H^+_{(aq)} + OH^\bullet$$
$$(3) \quad e^-_{aq} + H_2O \rightarrow H_2O^-$$
$$(4) \quad H_2O^- + H_2O \rightarrow H^\bullet + OH^-$$
$$(5) \quad H^\bullet + H^\bullet \rightarrow H_2$$
$$(6) \quad OH^\bullet + OH^\bullet \rightarrow H_2O_2$$
$$(7) \quad H^\bullet + OH^\bullet \rightarrow H_2O$$
$$(8) \quad H^\bullet + H_2O \rightarrow H_{2\,+}OH^\bullet$$
$$(9) \quad H_2O_2 + OH^\bullet \rightarrow H_2O + HO_2^{\,\bullet}$$
$$(10) \quad H^\bullet + O_2H^\bullet \rightarrow HO_2^{\,\bullet}$$
$$(11) \quad HO_2^{\,\bullet} + H^\bullet \rightarrow H_2O_2$$
$$(12) \quad R^\bullet + O_2 \rightarrow RO_2^{\,\bullet}$$

The Fricke dosimeter systems provides a reliable mean of absorbed doses measurement of in water, based on a process of oxidation of ferrous ions to ferric ions in acidic aqueous solutions by ionizing radiation [29].

When the gamma radiation interacts with Fe^{2+} ions transforms them into Fe^{3+} ions. The involved reactions are:

$$(1) \quad Fe^{2+} + OH^{\bullet} \rightarrow Fe^{3+} + OH^{-}$$
$$(2) \quad H^{\bullet} + O_2 \rightarrow HO_2^{\bullet}$$
$$(3) \quad Fe^{2+} + HO_2^{\bullet} \rightarrow Fe^{3+} + HO_2^{-}$$
$$(4) \quad HO_2^{-} + H^{+} \rightarrow H_2O_2$$
$$(5) \quad Fe^{+2} + H_2O_2 \rightarrow Fe^{3+} + OH^{-} + OH^{\bullet}$$

Each hydrogen atom forms a hydroperoxy radical, HO_2, and each of these radicals oxidizes three Fe^{2+} ions; one by reaction (3) and two by reactions (4), (5) and (1). Each hydroxyl radical oxidizes one Fe^{2+} ion, and each hydrogen peroxide molecule oxidizes two Fe^{2+} ions All reactions, except (5) are fast [32]. The organic impurities presence in the solution cause significant variation in the dosimeter response, for this reason it is essential to use very pure compounds.

Conventional Fricke dosimeter modified with gelatinous agent and the technique of image generation for Magnetic Resonance (MRI) has been used in dosimetric practices. The change of longitudinal proton relaxation time, T_1, due to the oxidation of ferrous ions (Fe^{2+}) to ferric ions (Fe^{3+}) in Fricke gel dosimeter after irradiation can be used for the dose distributions 3D determination [50-57].

An encapsulated liquid can be used in the dose control in irradiation process. If the reaction products radiation induced are stable and the changes in the color can be direct measured, with consequent variation in the optical absorption, and it is associated with the absorbed dose, this solution can be used us a dosimetric system. Dyed liquid systems have an advantage of being commercially available, cheap and easily handled, prepared and measured. The bromocresol green solution, an indicator of reaction, was prepared and characterized as a radiochromic dosimeter.

Methodology

Dosimeters Preparation

Potassium Nitrate

Pellets of KNO3 pure with different mass were cold pressed and the dosimetric properties were analyzed. It is known that same additives can increase the useful dose range of KNO_3 dosimeters. For this reason addition of compounds such potassium bromide (KBr), barium nitrate ($Ba(NO_3)_2$) and manganese dioxide (MnO_2) were studied. The *potassium nitrate pure* in powder form was dried in an oven at $80^{o}C$, samples were prepared by mixing required weights of each compound and grinding in agate mortar to obtain uniform grain size of 80 mesh. The homogeneous mixture was cold pressed in pellet form with diameter of 6 mm, using a Fred Frey press (model FC5; n° 2715) with applied load of 5 tons. The composition of the different mixtures is presented in the Table 1(a), (b), (c) and (d). Before irradiation the pellets were set in a badge, Figure 1, that consists of 2 Lucite® plates of 3 mm thick, that guarantee the electronic equilibrium condition to ^{60}Co gamma radiation, and 1 Lucite® plate of 1 mm thick with three holes, where the pellets are placed.

Table 1. Pellets composition of mixtures different of KNO_3 and additives.

(a)		
Pellet Mass (mg)	**-**	**KNO_3 %**
50	-	100
75	-	100
100	-	100
(b)		
Pellet mass (mg)	**MnO_2 %**	**KNO_3 %**
55.5	10	90
62.5	20	80
71.4	30	70
50.0	40	60
50.0	50	50
50.0	60	40
(c)		
Pellet mass (mg)	**KBr %**	**KNO_3 %**
50	40	60
50	50	50
50	60	40
(d)		
Pellet mass (mg)	**$Ba(NO_3)_2$ %**	**KNO_3 %**
50	40	60
50	50	50
50	60	40

(a) KNO_3 pure
(b) $KNO_3 + MnO_2$
(c) $KNO_3 + KBr$
(d) $KNO_3 + Ba(NO_3)_2$
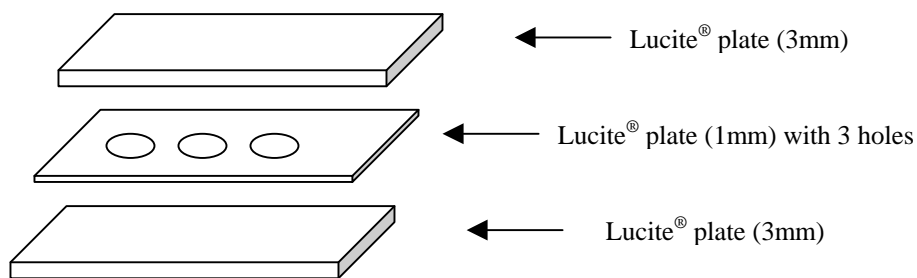
Figure 1. Schematic representation of the KNO_3 badge.

Bromocresol green solutions - VBC

The VBC is used in chemical analyses as acid - basic indicator and presents color change from yellow (pH 3,8) to blue (pH 5.4). Solutions with different VBC concentrations, 0.01%, 0.0075% and 0.005% in mass were prepared and evaluated. The indicator was dissolved in 5% ethyl alcohol and then added in right pureness water in the desired concentration. After dissolution the solutions were conditioned in amber glass bottles and stored in dark environment and room temperature.

Polimethylmethacrylate

A private firm using the dyes yellow, green, blue and red from Bayer produced PMMA sheets (120x60 cm^2 and thickness between 2 to 2.5 mm) especially to be used in this work. The PMMA sheets were cut into strips (10 mm width and 30 mm length) and sealed in special aluminum / paper / polyethylene pouches. The commercial Red 4034 Perspex and Gammachrome YR dosimeters were used for comparison with the new PMMA dosimeters.

Fricke gel dosimeter (FXG)

The Fricke gel (FXG) solutions were prepared using 50 mM sulphuric acid, 1 mM ferrous ammonium sulphate, 1 mM sodium chloride, 0.1 mM xylenol orange and 5% of porcine gelatine 270 Bloom. Sealed acrylic cuvettes of 10 mm optical path, 45 mm height, 1 mm wall thickness filled with Fricke gel solutions were used to calibrate the spectrophotometric and MRI signal intensity. A phantom in the breast shape was produced with FXG solution. The samples were always stored in dark environment at 5°C during 12 h to complete solidification.

Irradiation Facilities

Most of the irradiations were performed in electronic equilibrium conditions and room temperature and humidity using a Gammacell 220 source (38,9 x 10^{13} Bq) and a JOB-188 Dynamitron Inc. electron accelerator installed at the Radiation Technology Center CTR / IPEN-CNEN/SP.

Nitrate Potassium

Irradiations were performed using a ^{60}Co Gammacell source in the dose range between 1 and 150 kGy. The dose rate was approximately 7,48 kGy /h. The dose rate can be changed depending on the distance source-dosimeter.

Bromocresol green solutions

The solutions were irradiated in air at electronic equilibrium conditions with ^{60}Co Gammacell radiation and doses between 50 Gy and 15 kGy.

Polymethylmethacrylate

The PMMA dosimeters were irradiated with ^{60}Co Gammacell and electron from accelerator in air at electronic equilibrium. The absorbed dose rate corresponding to 4.9 kGy/h, was determined by Fricke dosimeter in the Gammacell source.

Fricke gel dosimeter

The gamma irradiations were performed in air at electronic equilibrium conditions using a Gammacell source with doses between 5 and 50 Gy and dose rate of 3.28 kGy/h.

Dose Evaluation

Each related point is the average of 3 measurements and the error bars the standard deviation of the mean (1σ).

Nitrate Potassium

For optical measurements potassium nitrate pellets were dissolved in 50 mL of high purity water in a 100 mL volumetric flask. After dissolution 20 mL of a coloring solution, composed by solutions A and B in the proportion of 5:1 was added. The solution A was prepared dissolving 2 g of sulfanilamide p.a. in l L of 30% of glacial acetic acid p.a. solution and solution B was prepared dissolving 1 g of N – 1 - Naphtylethylene - diamine dihydrochloride p.a. in 1 L of 30% of glacial acetic acid p.a. solution. Ten minutes after dissolution the absorbance was measured at 546 nm wavelength [58,59]. The absorbance of the solutions of irradiated and non-irradiated pellets of KNO_3 was measured against air, at the wavelength range from 500 to 600 nm using a Shimadzu UV1601PC (potassium nitrate pure) and UV-2101PC (mixtures) spectrophotometer.

Bromocresol green solutions

The solutions were evaluated immediately after irradiation using a Shimadzu UV1601PC spectrophotometer.

Polymethylmethacrylate

The absorbance changes were measured immediately after irradiation with a Shimadzu UV-2101PC spectrophotometer at the wavelength of maximum absorbance or maximum transmittance, depending on the dosimeter absorption spectrum at the wavelength range from 190 to 900 nm.

Fricke gel dosimeter

The Fricke gel solutions were measured immediately after irradiation using Shimadzu UV2101PC spectrophotometer at the wavelength from 190 to 900 nm. The MRI were obtained using a Philips Gyroscan S15/ACS (1.5 T) tomography and quadrature body coil using the IR sequence with following parameters: TR=367 ms, TI=300 ms and TE=18 ms.

Results

Potassium Nitrate

The dosimeter composed of pure potassium nitrate presents useful dose range between 5 and 150 kGy. The calibration curve of the dosimeter irradiated with gamma radiations is shown in Figure 2.
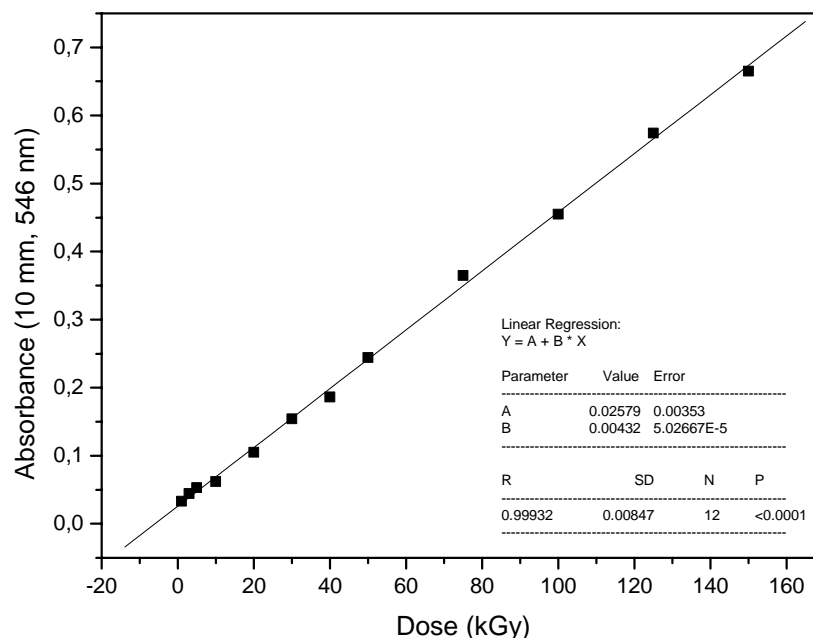
Figure 2. Potassium nitrate dosimeter calibration curve. Irradiation - 60Co gamma radiation and measurement - 546nm.
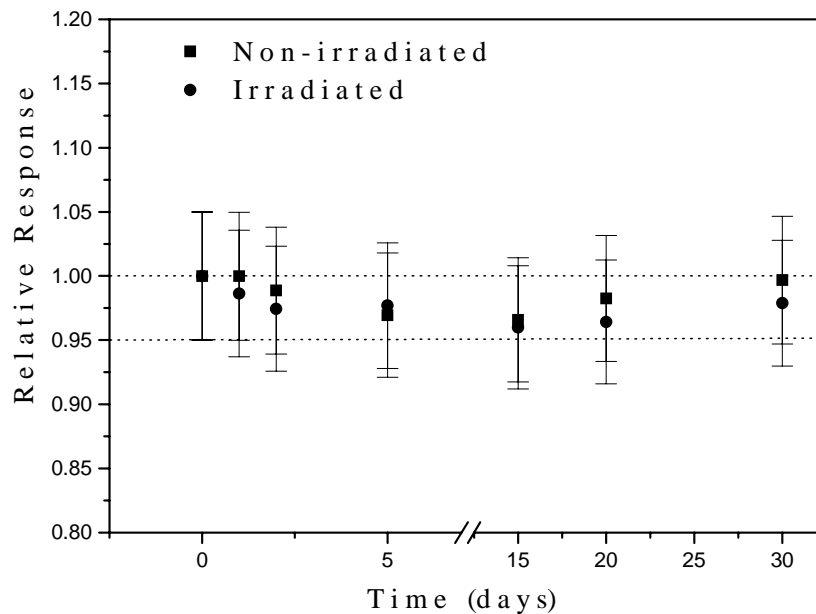
Figure 3. Relative response obtained with solutions (40% MnO_2 / 60% KNO_3) evaluated immediately after preparation and using pellets irradiated with 200 kGy and stored up to 30 days.

The maximum color intensity of the solution is obtained 10 minutes after preparation. The solutions are stable during a period of 1 h that permits the dose evaluation with high quality guarantee. The pellets irradiated and non-irradiated can be stored by long periods

without any change in their characteristics.The results obtained with solutions evaluated immediately after preparation, using pellets irradiated and stored up to 30 days are shown in the Figure 3. The results obtained with solutions prepared at same time and evaluated periodically during 1 month of storage are shown in the Figure 4.
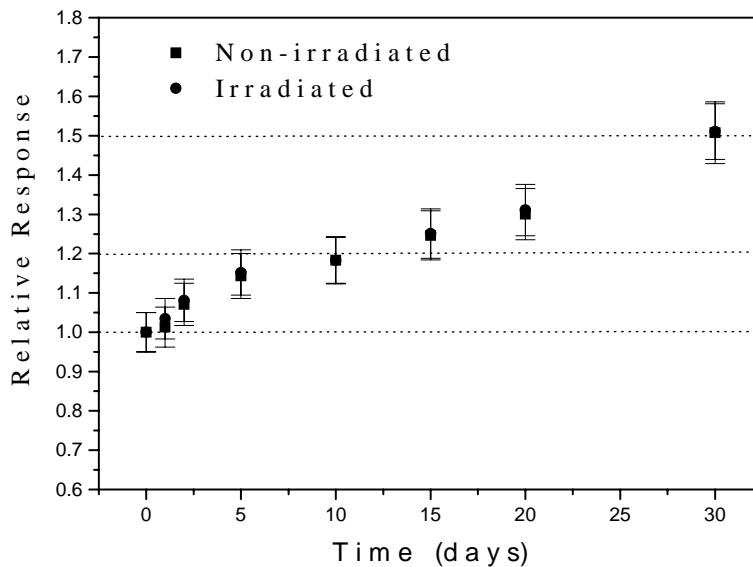
Figure 4. Relative response obtained with solutions prepared using pellets (40% MnO_2 / 60% KNO_3) irradiated with 200kGy, prepared and evaluated after up to 30 days of storage.
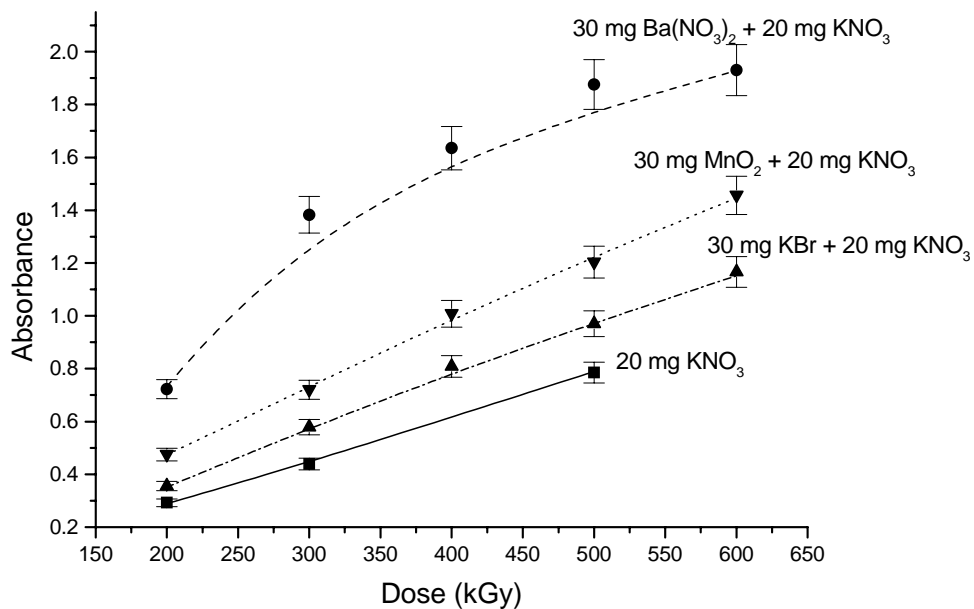
Figure 5. Dose-response (λ=540 nm) for mixtures of 30 mg $Ba(NO_3)_2$, KBr and MnO_2 and 20 mg KNO_3 irradiated with ^{60}Co gamma radiation.
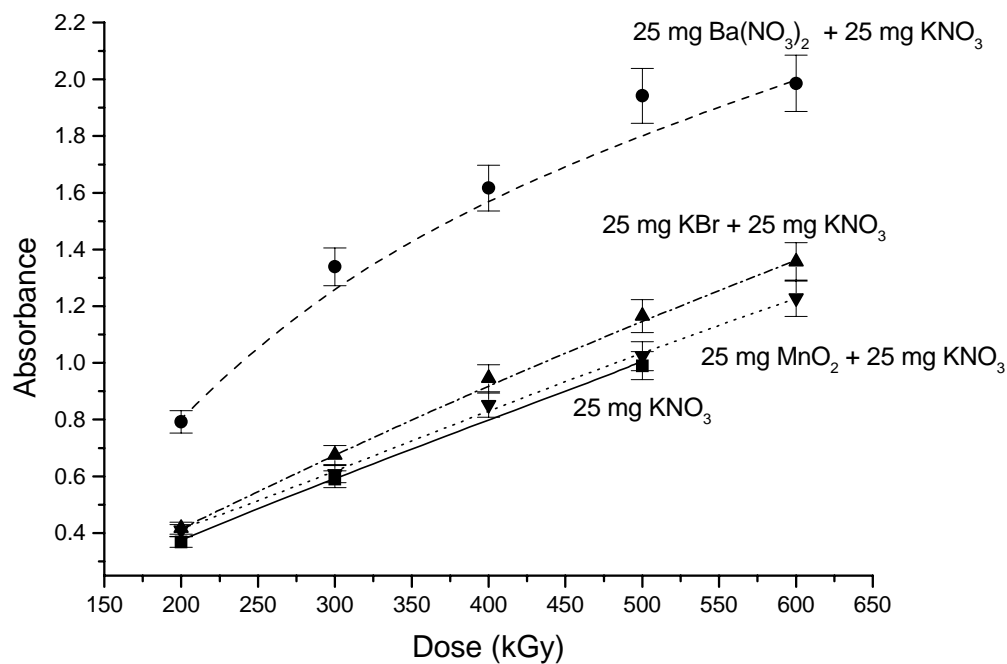
Figure 6. Dose-response (λ=540 nm) for mixtures of 25 mg $Ba(NO_3)_2$, KBr and MnO_2 and 25 mg KNO_3 irradiated with ^{60}Co gamma radiation.
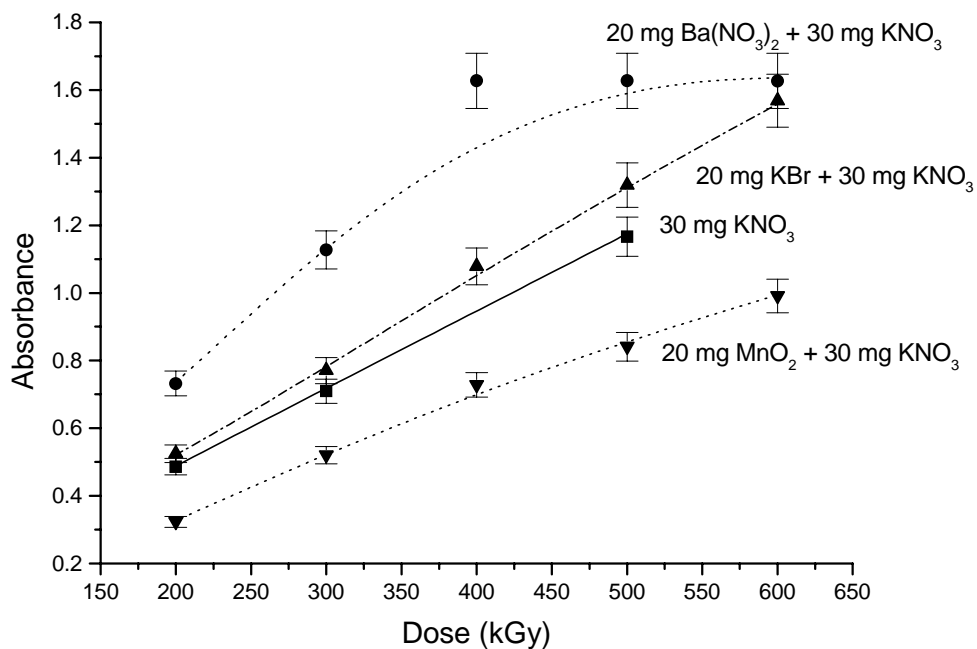
Figure 7. Dose-response (λ=540 nm) for mixtures of 20 mg $Ba(NO_3)_2$, KBr and MnO_2 and 30 mg KNO_3 irradiated with ^{60}Co gamma radiation.

The absorbance response of KNO_3 pure pellets and pellets of different compounds were evaluated for absorbed doses from 200 kGy to 600 kGy. The results are shown in Figures 5, 6 and 7 for the mixtures $Ba(NO_3)_2/KNO_3$, KBr/KNO_3 and MnO_2/KNO_3 in different concentrations.

The method reproducibility was studied preparing different batches of pellets and evaluating the optical response for different doses. The reproducibility was found to be better than 98% (1σ) from batch to batch.

The mixture of 20 mg MnO_2 / 30 mg KNO_3 presents better results in terms of decomposition rate. The decomposition rate of nitrate ions into nitrite ions is reduced, extending the useful range. In the case the dose range was extended up to 600 kGy, without signal saturation.

No dose rate dependence response in the range from 1.70 to5.65 kGy/h was observed. The fluctuation observed was better than 95%.

Polymethylmethacrylate

The absorption spectrum obtained from non-irradiated PMMA dosimeters are shown in Figure 8 (a), (b), (c) and (d).

The batch reproducibility was evaluated and was found to be better than 98% from batch to batch, represented by a sheet produced in the dimensions 60 x 120 cm^2.

The effects of room temperature, humidity and light on the dosimeters response were studied.

Different humidity conditions between 0 and 100% were obtained by means of saturated salt solutions that are very useful in producing known relative humidity. Non-irradiated samples were exposed, during several hours, to atmospheres with relative humidity (R.H.) of 0%, 75.5%, 93.0% and 100.0%. The samples that contains the green dye were the ones that presented smaller variation in the optical response, the absorbance intensity decrease was less than 2.5% however, significant variation was not observed in the other samples, the largest variation found was ± 5.0% for the red H and red G dyed samples, for the standard dosimeter was found ± 5.0% of variation for Red Perspex and an absorbance value decrease of 10.0% for Gammachrome YR. To determine the effect of R.H. on irradiated samples, the samples were exposed to different R.H. conditions during 24 hours and, after the exposition were irradiated in the Gammacell source with dose of 20 kGy, in the same R.H conditions. The obtained responses are shown in the Figure 9.

The non-irradiated and irradiated samples were submitted to thermal treatments of 4, 40, 80 and 100°C during one hour. After temperature stabilization the absorbance of the non-treated sample (samples maintained at room temperature) and treated samples were measured. In the Figure 10 and Figure 11 are shown the relative responses obtained for non-irradiated and irradiated (20 kGy) PMMA samples, respectively. The presented values of each treated dye sample were normalized to the respective response of non treated sample.
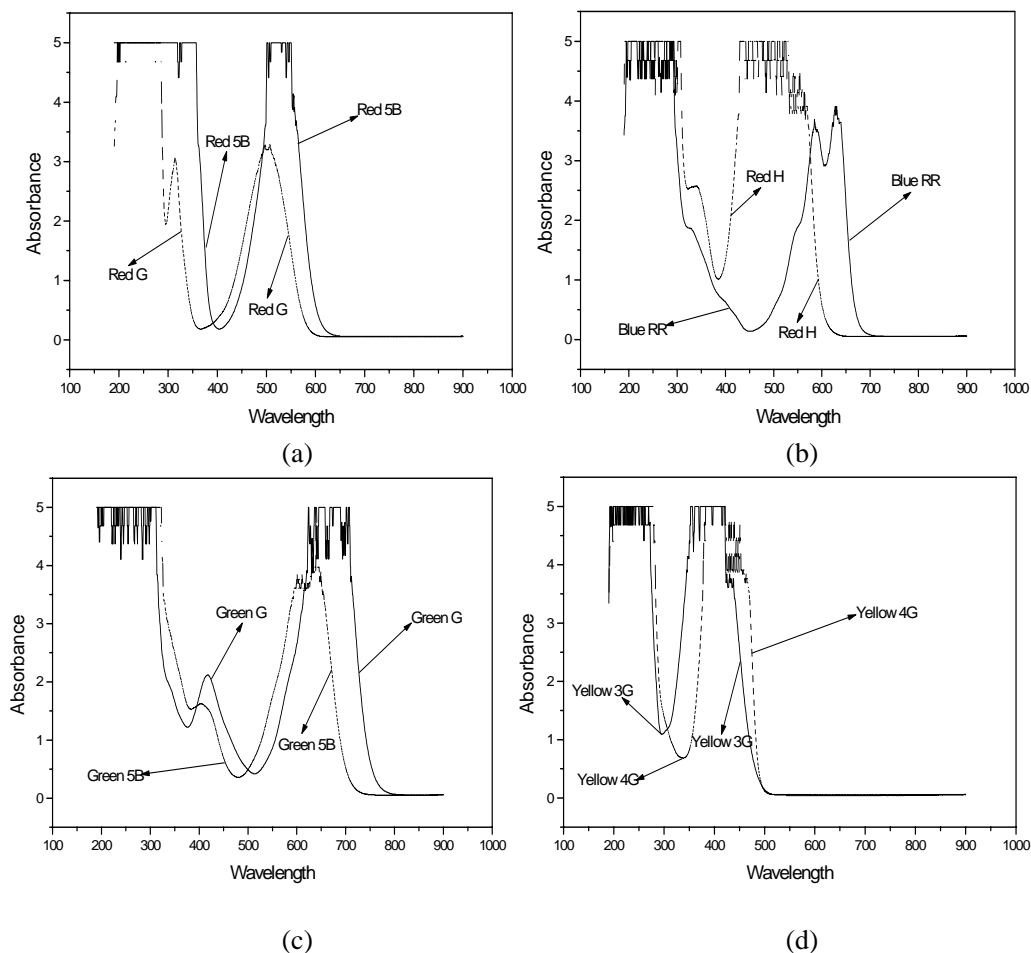
(a) Red 5B and Red G. (b) Red H and Blue RR. (c) Green 5B and Green G PMMA. (d) Yellow 3G and Yellow 4G PMMA.

Figure 8. Absorption spectrum of the non-irradiated dyed PMMA dosimeters.
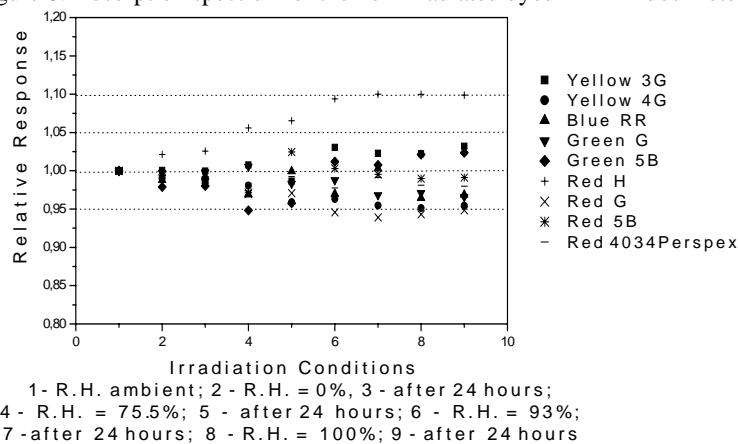

Figure 9. Relative response of the irradiated PMMA samples - dose 20 kGy of ^{60}Co gamma radiation as a function of relative humidity
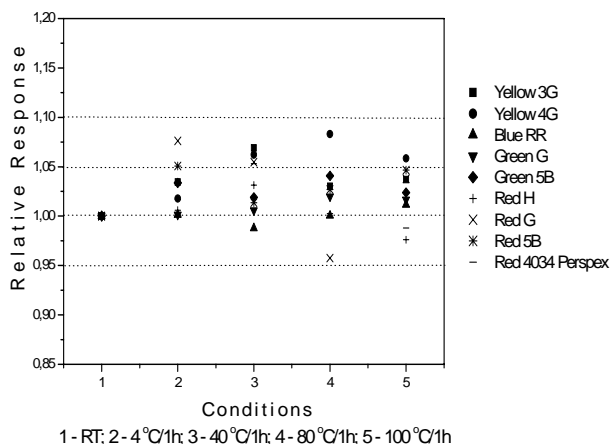
Figure 10. Optical response of non-irradiated PMMA samples maintained at room temperature (RT) and submitted to thermal treatments (TT) between 4 and 100°C /1h.
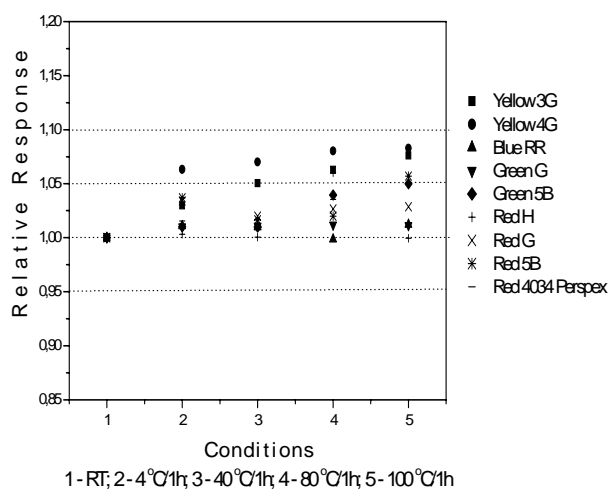

Figure 11. Optical response of irradiated PMMA samples - dose 20kGy maintained at room temperature (RT) and submitted to thermal treatments (TT) between 4 and 100°C /1h.

In the Figure 12 and Figure 13 are shown the relative responses obtained for non-irradiated samples exposed to ambient light, is observed an increase in the response of 5% in two months. Some materials are only photosensitive after irradiation, this way, it is necessary to determine how that factor can influence the performance of the dosimeter in order to avoid or to minimize this influence in the response. The PMMA samples were irradiated using the Gammacell source with doses of 10, 30 and 40 kGy and exposed to the laboratory ambient light. The samples presented media variation of ± 10% in the response, in that way the effect of the incident light in the irradiated samples is significant and appropriate careful has to be taken, packing the dosimeter for instance or applying correction factors. To avoid the application of corrections factors the samples has be maintained in a dark ambient and the measuring realized soon after irradiation or in the maximum between 1 or 2 days after irradiation.
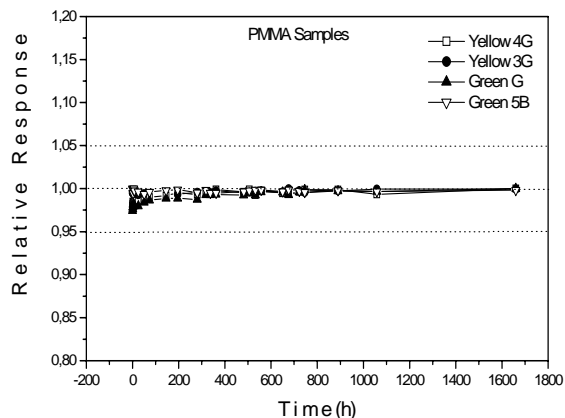
Figure 12. Relative response of non-irradiated PMMA samples – dyed with yellow 4G, yellow 3G, green G and green 5B – exposed to ambient light.
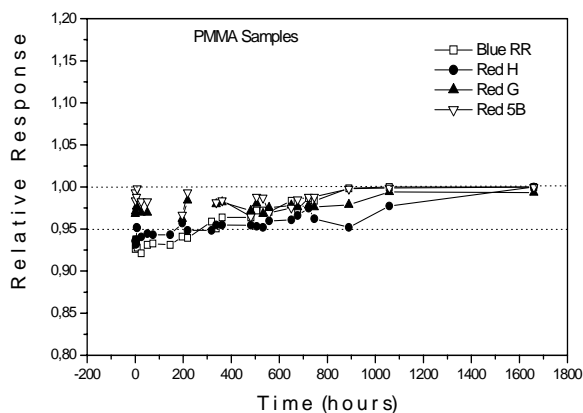

Figure 13. Relative response of non-irradiated PMMA samples – dyed with blue RR, red H, red G and red 5B – exposed to ambient light.

The dosimeters did not present significant variation on the absorbance response when exposed to the normal conditions of light and temperature, therefore, can be manipulated without special care. Although the dosimeters have not presented significant variation on the absorbance response for the different humidity conditions it is desirable that the dosimeters are maintained sealed in pouches.

Figure 14 (a), (b), (c), (d), (e), (f), (g) and (h) show dose-response curves to ^{60}Co gamma irradiation with doses between 0.5 and 100 kGy of the PMMA dosimeters produced with dyes yellow 3G, yellow 4G, blue RR, green G, green 5B, red H, red G and red 5B measured at 300 nm, 353 nm, 450 nm, 528 nm, 405 nm, 620 nm, 397 nm and 415 nm, respectively.

The wavelengths of yellow 3G, yellow 4G, blue RR, green G and red 5B PMMA dosimeters were taken from transmittance spectrum and green 5B, red H and red G PMMA dosimeters were taken from absorbance spectrum. The selected wavelengths presented higher sensitivity as a function of the dose and better stability as a function of environmental conditions.
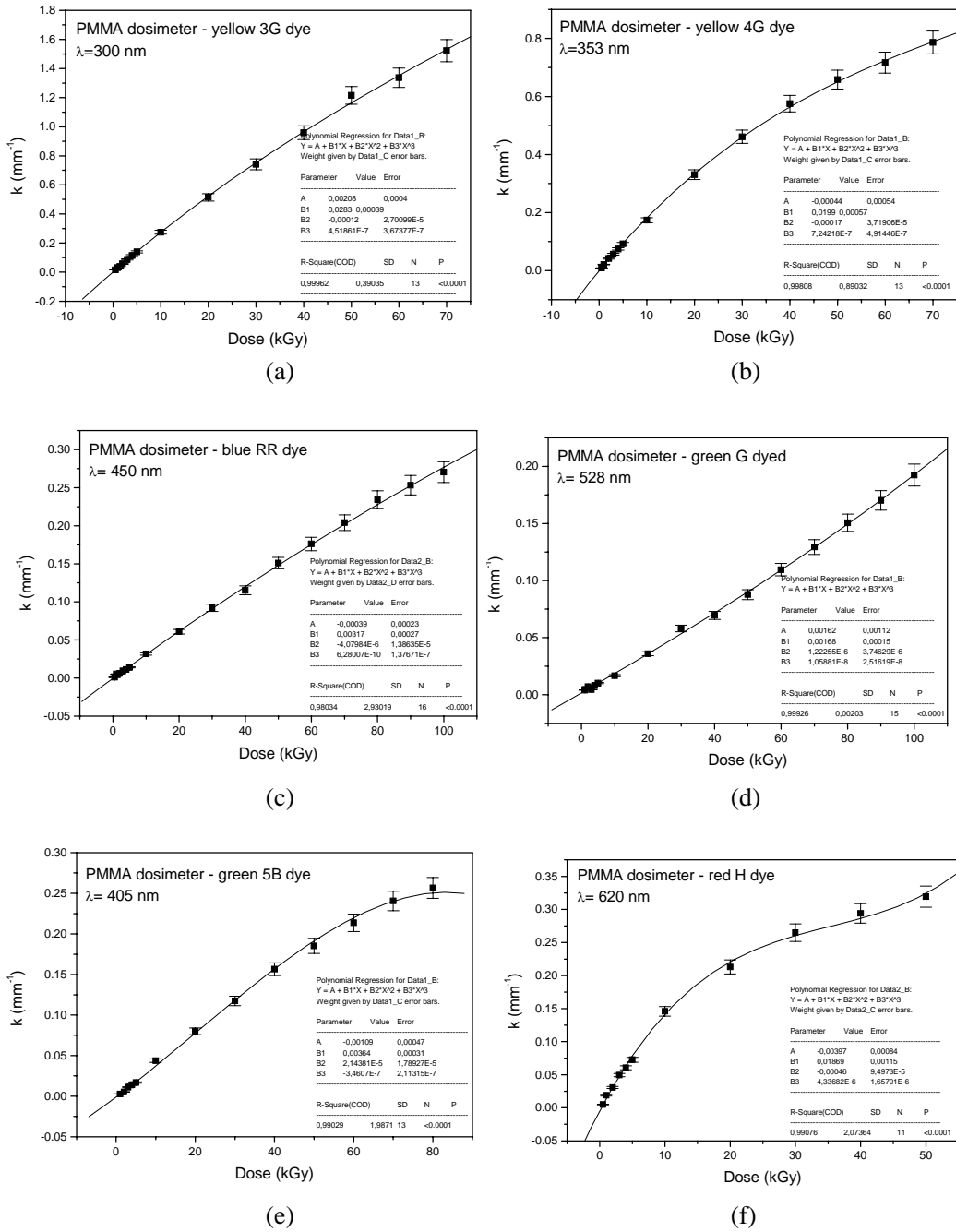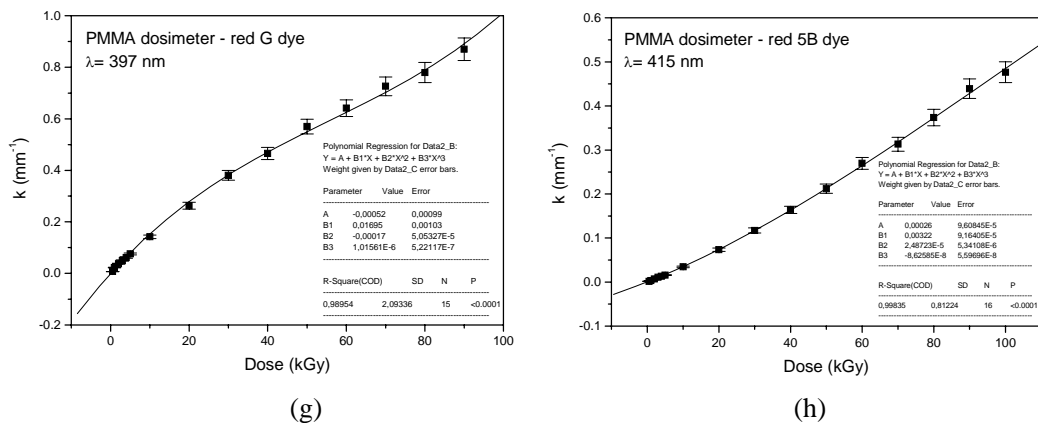
Figure 14. Continued on next page.

(g)

(h)

Figure 14. Dose-response curves for PMMA dosimeters irradiated with ^{60}Co gamma radiation.
(a) Yellow 3G, λ = 300 nm. (b) Yellow 4G, λ = 353 nm. (c) Blue RR, λ = 450 nm. (d) Green G, λ = 528 nm. (e) Green 5B, λ = 405 nm. (f) Red H, λ = 620 nm. (g) Red G, λ = 397 nm. (h) Red 5B, λ = 415nm.

Using lead attenuators, the samples were irradiated with 20 kGy of ^{60}Co gamma radiation with dose rates 4.90 kGy/h (without attenuator); 2.45 kGy/h (50% attenuation); 1.47 kGy/h (70% attenuation) and with 0.49 kGy/h (90% attenuation). The relative response of the dosimeters was determined in terms of the absorbance value by thickness unit normalized to the lower dose-rate. The samples containing the yellow 4G, green G, green 5B, red H and red G dye presented behavior similar to the comparative standard Red 4034 Perspex (variation between 5-10%). For the samples containing the yellow 3G, blue RR and red 5B dye the found variation is of approximately 20%, Figures 15 and 16, respectively.
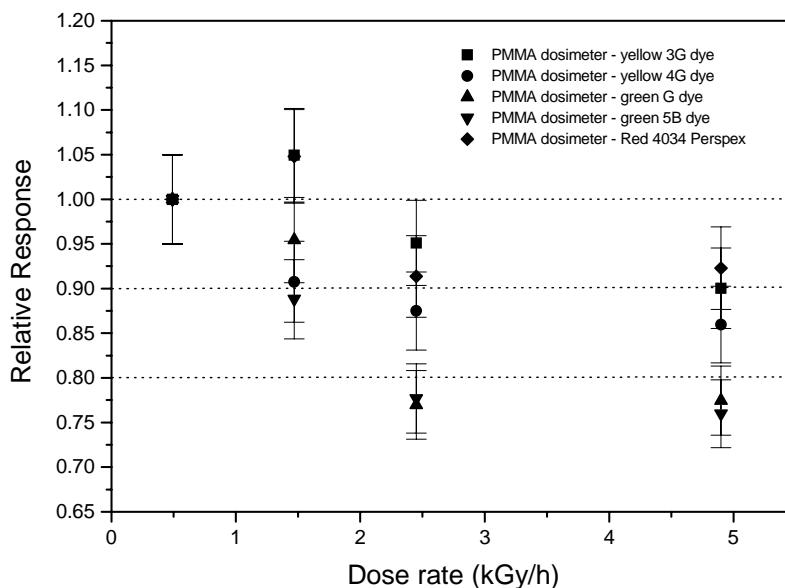

Figure 15. Absorbance dose-rate response of dyed PMMA dosimeters yellow 3G, yellow 4G, green G and green 5B: dose 20 kGy.
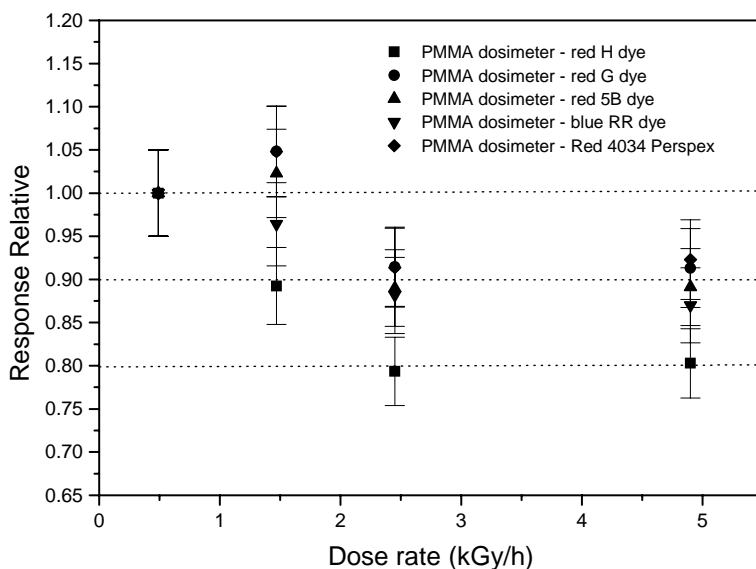
Figure 16. Absorbance dose-rate response of dyed PMMA dosimeters red H, red G, red 5B and blue RR: dose 20 kGy.

The dose response curves of the detectors produced with yellow 3G, yellow 4G, blue RR, green G, green 5B, red H, red G and red 5B, measured at 300 nm, 353 nm, 450 nm, 528 nm, 405 nm, 620 nm, 397 nm and 415 nm, respectively, irradiated in the electron accelerator (energy 1.25 MeV and current 0.6 mA) at doses between 1.2 and 110 kGy are presented in Figure 17 (a), (b), (c), (d), (e), (f), (g) and (h), respectively.

To analyze the electron dose-rate dependence response the samples were irradiated with dose rates 2.66 kGy/s, 22.61 kGy/s and 45.22 kGy/s with electron energy of 1.25 MeV obtained varying the current between 0.6 e 10.2 mA. The results obtained are shown in Figure 18 (a) and (b). The relative response of the detectors was determined in terms of the value of the absorbance by thickness unit normalized to the lower dose-rate.
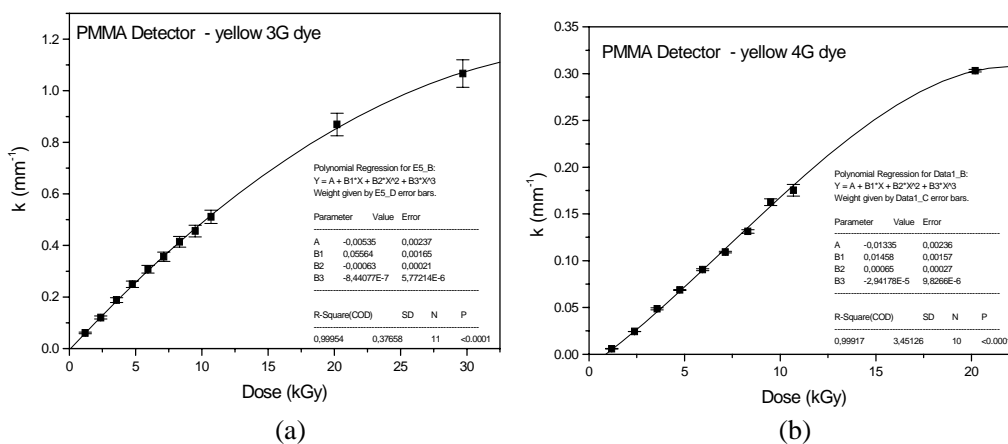

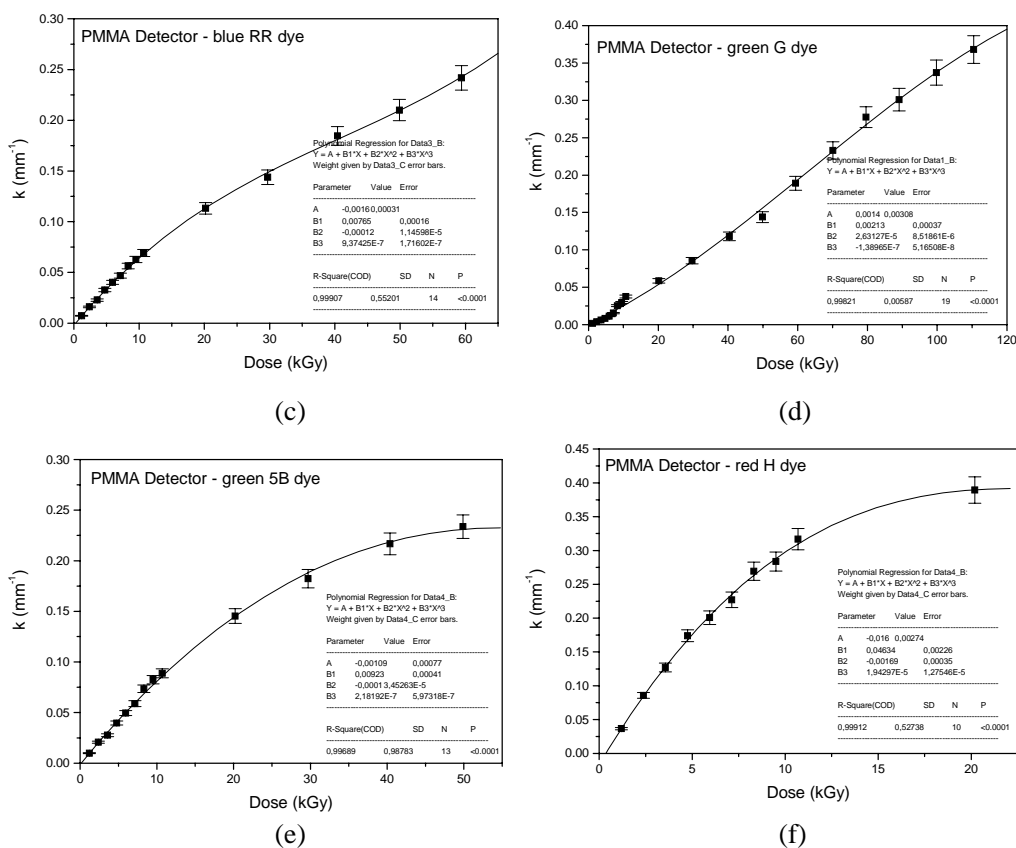(a)   (b)

Figure 17. Continued on next page.

(c)

(d)

(e)

(f)

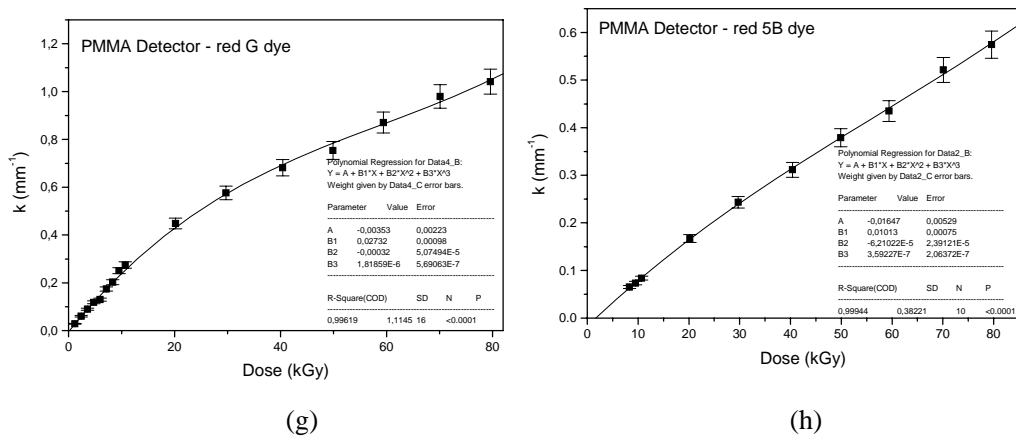Figure 17. Continued on next page.

(g)

(h)

Figure 17 (cont.). Dose-response curves for PMMA detectors irradiated with 1.25 MeV electrons (JOB188).

(a) yellow 3G PMMA detector, at 300 nm. (b) yellow 4G PMMA detector, at 353 nm. (c) blue RR PMMA detector, at 450 nm. (d) green G PMMA detector, at 528 nm. (e) green 5B PMMA detector, at 405 nm. (f) red H PMMA detector, at 620 nm. (g) red G PMMA detector, at 397 nm. (h) red 5B PMMA detector, at 415nm.
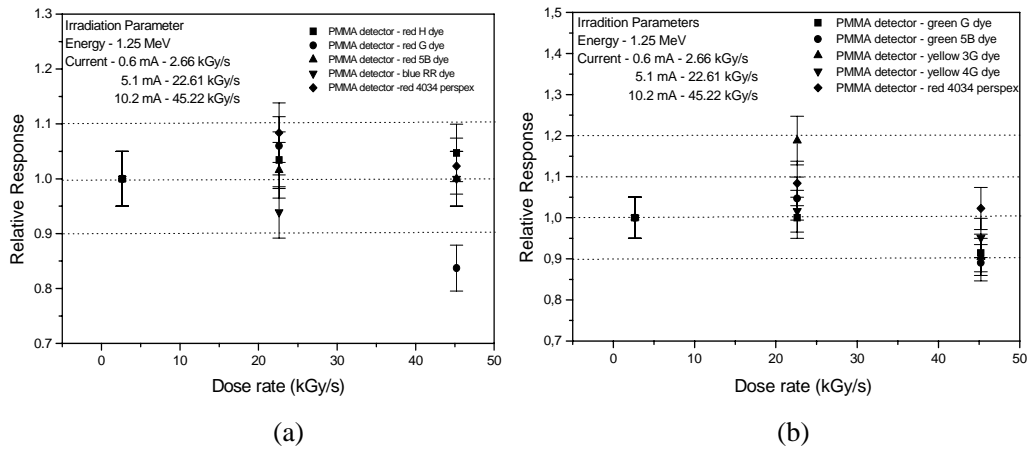
Figure 18. Electron dose-rate dependence response. (a)PMMA detectors – Dye red H (λ=620 nm); dye red G (λ=397 nm); dye red 5B (λ=415 nm) and dye blue RR (λ=450 nm); red 4034 Perspex. (b) PMMA detectors – Dye yellow 3G (λ=300 nm); dye yellow 4G (λ=353 nm); dye green G (λ=528 nm) and dye green 5B (λ= 405 nm); red 4034 Perspex.

The electron energy dependence response was determined using samples 2.4 mm thick. The samples were irradiated with electron energies of 0.8, 1.25 and 1.5 and current of 0.6 mA. The results obtained are show in Figure 19 (a) and (b). For measurements using detector thickness of 1.2, 2.5, 3.1, 4.3 and 5.6 mm and electron energies of 0.8, 1.25, 1.5 MeV no energy dependence was observed when the thickness was maintained inside of the electron range. The relative response of the detectors was determined in terms of absorbance value by thickness unit normalized to the lower energy.
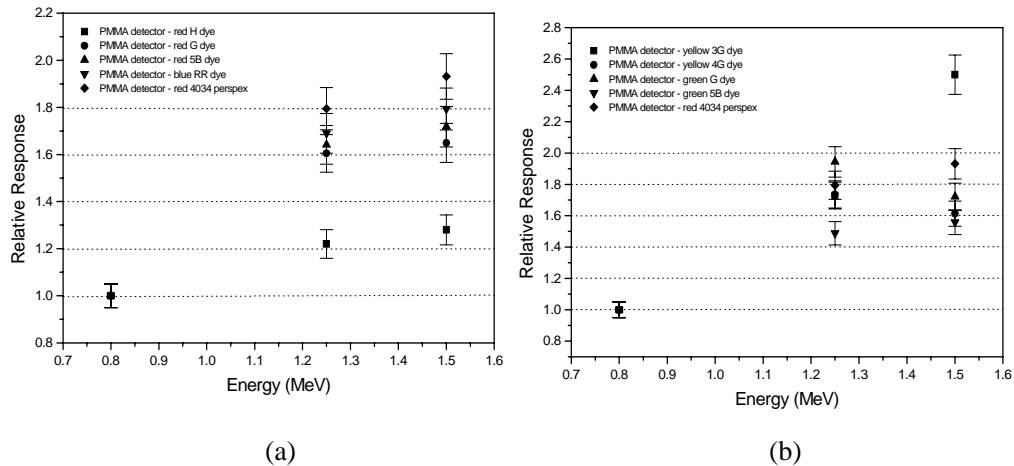

Figure 19. Electron energy dependence response. (a)PMMA detectors – Dye red H (λ=620 nm); dye red G (λ=397 nm); dye red 5B (λ=415 nm), dye blue RR (λ=450 nm) and red 4034 Perspex (λ=640 nm). (b) PMMA detectors – Dye yellow 3G (λ=300 nm); dye yellow 4G (λ=353 nm); dye green G (λ=528 nm), dye green 5B (λ= 405 nm) and red 4034 Perspex (λ=640 nm).

The absorption spectra of non-irradiated solutions prepared with different bromocresol green concentrations between 0.005 and 0.01% are shown in Figure 20, two absorption bands with maximums at 450 and 620 nm can be observed.
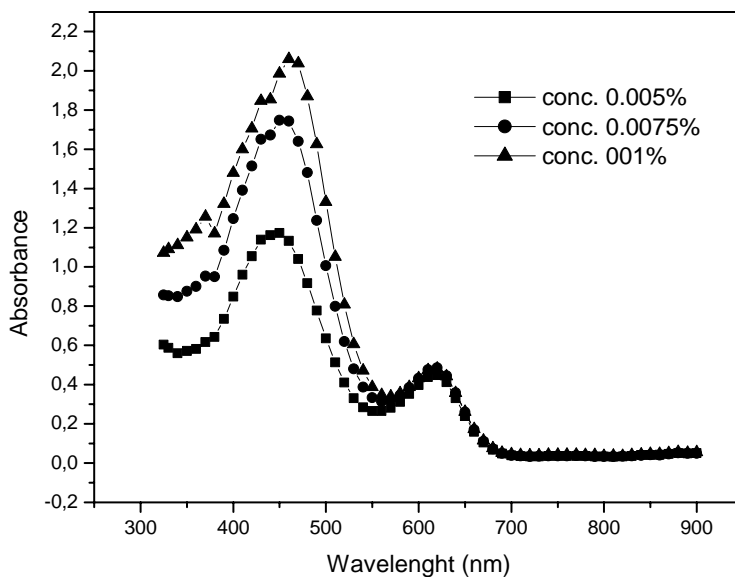
Bromocresol green

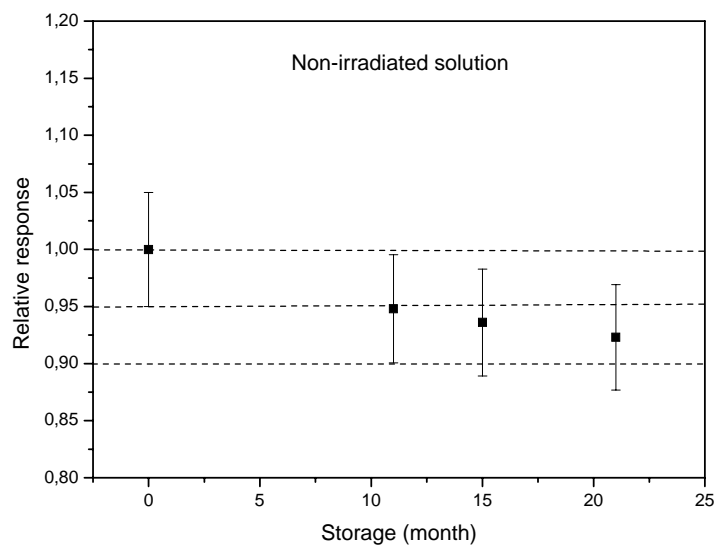Figure 20. Bromocresol green aqueous solution absorption spectra: non-irradiated samples.

Figure 21. Response stability of non-irradiated bromocresol green solution at room temperature.

Non-irradiated aqueous solutions of bromocresol green were stored during 21 months under room temperature and evaluated in different times after preparation. No significant variations were observed as shown in the Figure 21. These results indicate that it is not

necessary fresh solutions for each experiment, the solutions are stable for longer storage time. The post-irradiation stability was observed during a period of about 48 hours, no absorbance change larger than 3% was observed, Figure 22.
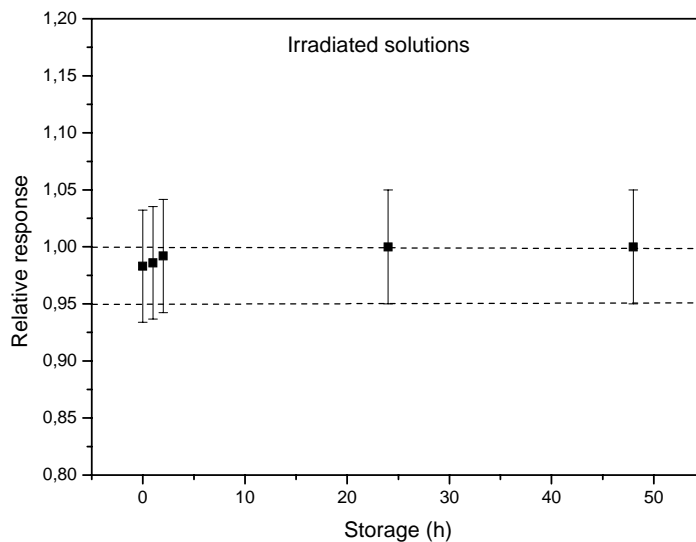

Figure 22. Post-irradiation response of bromocresol green solutions irradiated with gamma radiation with 8 kGy and storage during 48 hours.

The absorbance values of the 0.075% bromocresol green solutions was plotted as a function of absorbed dose between 50 Gy and 15 kGy at 450nm. A grade extinction of optical absorption intensity is shown in Figure23 and a linear response in the studied range is observed.
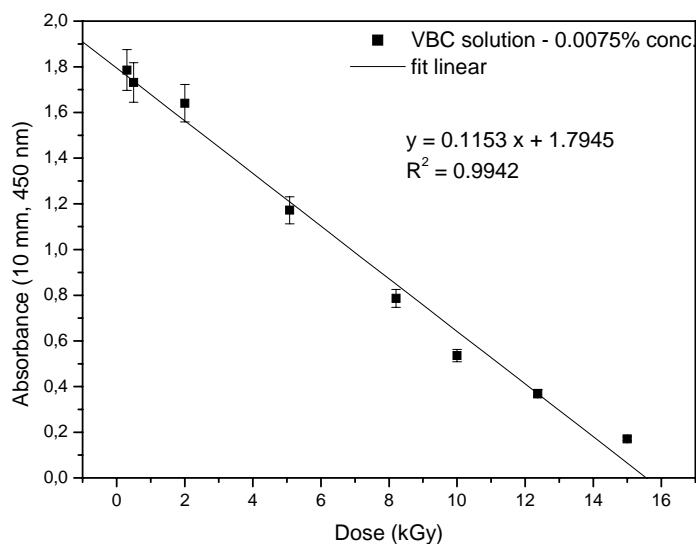

Figure 23. Dose response curve of 0.0075% bromocresol green solution.

Fricke gel (FXG)

Spectrophotometric measurements in the wavelength range between 190 and 900 nm were performed for non-irradiated Fricke gel samples. In the Figure 24 is shown the spectrum obtained in the range 350-650 nm. The non-irradiated (0Gy) gel sample presents two absorption bands at 440 and 585nm originated by Fe^{2+} and Fe^{3+} presence respectively in the sample.
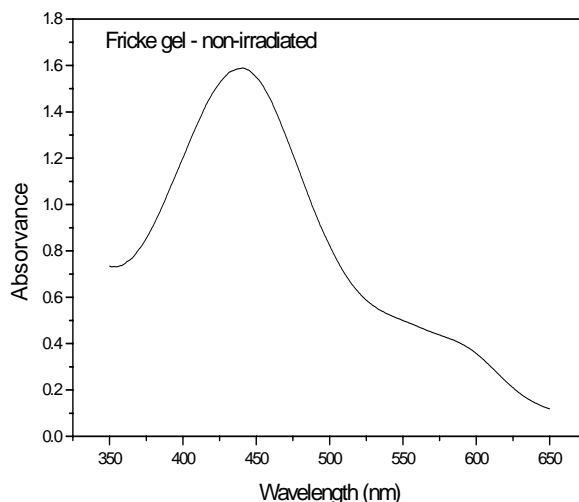

Figure 24. Non-irradiated Fricke gel spectrum: wavelength range 350 - 650 nm.

Absorption spectrum of irradiated FXG solutions with doses between 5 and 40 Gy were recorded in the range of 400 and 625 nm and presents the same two bands; in this case the 585 nm band increases with the dose (Fe^{3+} increasing concentration) and the 440 nm band (Fe^{2+} decreasing concentration) tends to disappear. In the Figure 25 is shown the spectra of Fricke gel solutions as a function of the ^{60}Co radiation dose.
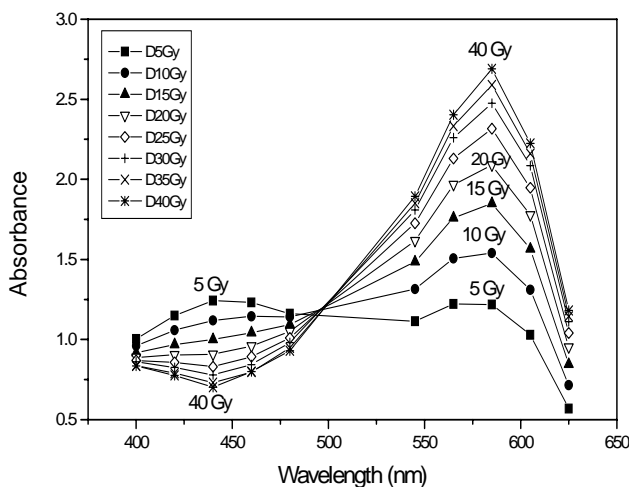

Figure 25. Fricke gel spectrum. Gamma doses between 5 – 40 Gy, wavelength range between 400 and 625 nm.

In the Figure 26 is shown the dose-response curve of Fricke gel samples irradiated with doses between 5 – 40 Gy of ^{60}Co gamma radiation. The 0 Gy absorbance value of 585 nm band (Fe^{3+}) was subtracted. The obtained results are close with that presented by Bero [50-51].
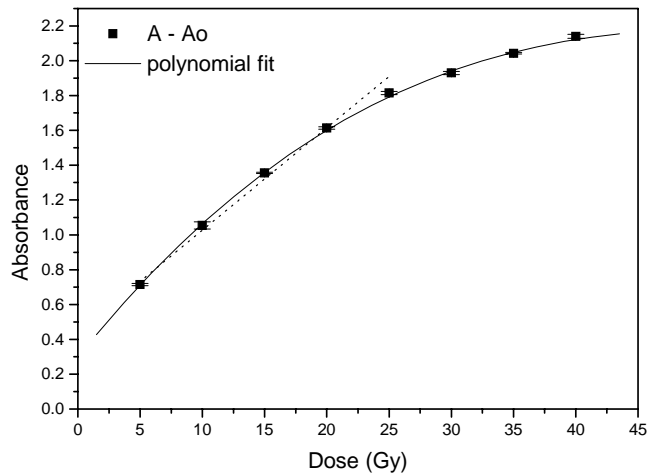

Figure 26. Dose-response curve of Fricke gel dosimeter irradiated with ^{60}Co gamma radiation.

Brest simulators were prepared using the gel solution and preliminary measures using spectrophotometry technique were performed introducing the cuvettes containing the gel solution in the simulator. Figure 27 (a) and (b) shows the breast phantom and the dosimeter positioning, respectively.

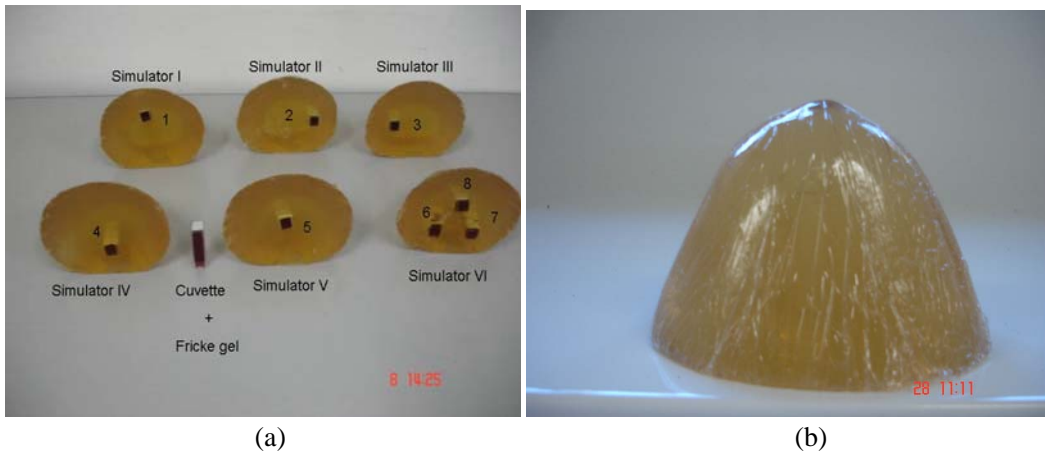(a)   (b)

Figure 27. Breast simulators 340ml (a) simulator and (b) dosimeter positioning.

The simulator was irradiated with 15Gy at point 2. The obtained values obtained was 15.2Gy at point 2 and 12.21Gy at point 1 This result shows that the dosimeter presents good sensitivity and can be used to dose distribution determination.

Spectrophotometric analysis has proved to be very reliable. Moreover, Nuclear Magnetic Resonance (NMR) analysis gives the possibility of spatial determination of paramagnetic species, because of influence of the ferric ions on the spin relaxation times of the hydrogen nuclei of the solution.

Changes in proton relaxation time related with absorbed dose due ferric ion presence were determinate using samples irradiated with 20 Gy and measures performed using a Gyroscan S 15/ASC (1.5T) equipment. A linear relation was found between the relaxation rate of the solution and the absorbed dose. The correlation coefficient was 0.99 shown in the Figure 28.
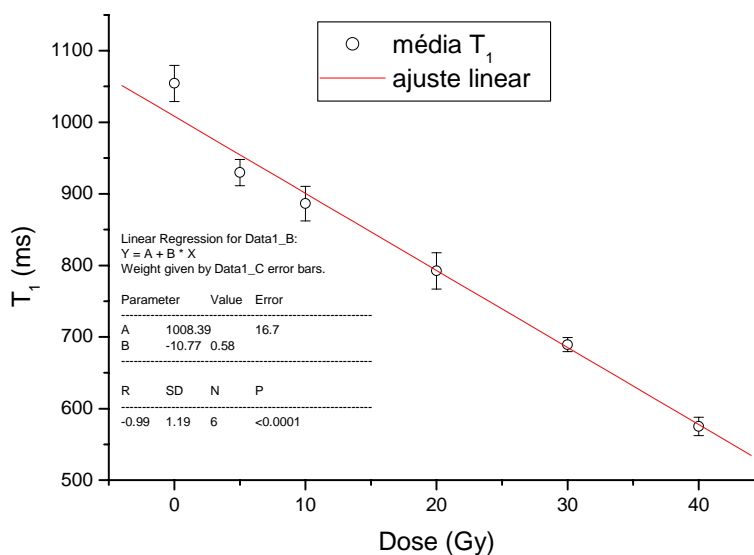
Figure 28. Proton relaxation time as a function of absorbed dose for FXG solution.

Coronal plane   sagital plane   axial plane
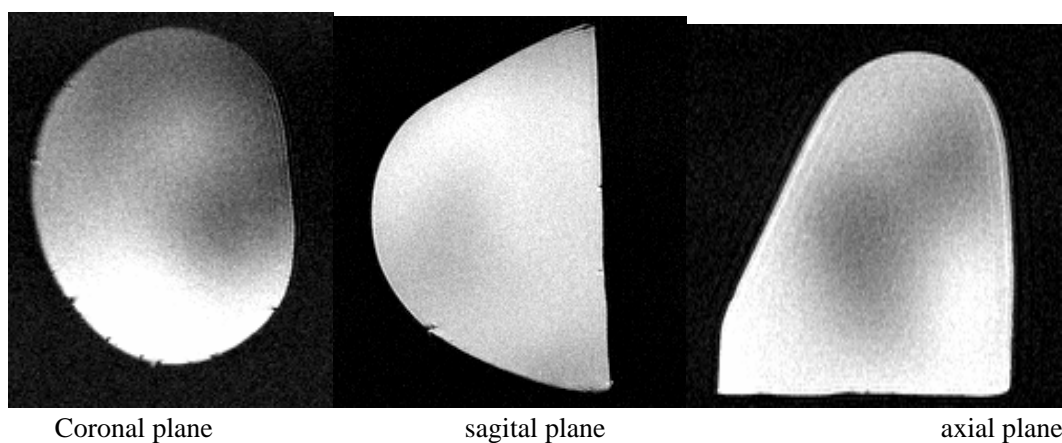
Figure 29. Magnetic resonance image to FXG breast simulator irradiated with ^{60}Co gamma radiation.

Preliminary magnetic resonance images were performed using a breast simulator prepared with Fricke gel solution, Figure 29. Changes in the image intensity are observed as a result of the dose distribution on the simulator. The brightness area corresponds with the

higher absorbed dose. Dose calibrations are in gray scale and color scale are in progress aiming to construct the isodose curves.

Conclusion

The potassium nitrate can be used in pellet form for irradiation and processed for optical measures in the solution form. Environmental conditions do not affect the response, but the pellets should be maintained sealed and handled in humidity atmosphere below 60%. The dosimetric properties of this compound are appropriated for high doses applications. The system presents a reproducible response in the dose range between 1 and 150 kGy. The addition of MnO_2 in the pellet composition increase dose range for 600kGy.

The use of dyed PMMA detectors for electron beam and gamma dosimetry is cheap and the absorbance analysis is very simple. The detectors are easy to prepare, manipulate and analyze. The useful dose range of the eight dyed PMMA detectors developed is large and interesting for dose evaluation in radiation processing and their performance is according to the commercially available Red 4034 Perspex detector. The yellow 4G, green G and red 5B detectors were shown to be the most promising, considering their response characteristics and dose range, although the others detectors can also be used for different dose ranges. All types of dyed PMMA detectors demonstrated high sensitivity and reproducibility. They do not present energy dependence when thicknesses equal to or smaller than the range of the electrons with different energies. These data also show that the dyed detectors present promising characteristics and can be useful for electron dosimetry.

Aqueous solution of bromocresol green can be used for a dose interval between 0.3 and 15 kGy. The solutions are stable and can be used after preparation for various months.

The FXG dosimeter is easy to prepare and cheap. The gelatine is tissue equivalent and can be prepared in a variety of the shapes and volumes. The effect of the natural oxidation needs to be known and separated of the contribution radiation induced. The best dosimeter storage condition is to maintain the solution at dark environment and low temperature ($5^{o}C$). The spectrophotometry technique is cheaper and faster than MRI technique and provides good results. The gel dosimeter can be also used to determination of absorbed dose distribution in radiotherapy treatments. The improvement of this technique using MRI will provide the obtaining of the isodose curves in the irradiated organ simulators.

All developed materials are available for high dose evaluation and can be used according to the characteristics of the installation, dose level required and material atomic number.

References

[1]   Martins, J. B. (2007). História da energia nuclear. Apostilas CNEN. Available from: http://www.cnen.gov.br.

[2]   McLaughlin, W. L.; Desrosiers, M. C. Dosimetry systems for radiation processing *Radiat Phys Chem*. 1995, 46, 4-6, 1163-1174.

[3]   Mehta, K.; Fuochi, P. G.; Kovacs A.; Lavalle M.; Hargittai P. Dose distribution in electron-irradiated PMMA: effect of dose and geometry. *Radiat Phys Chem*. 1999, 55, 773-779.

[4] Regula D. F.; Deffener, U. Dosimetry by ESR spectroscopy of alanine. *Int J Appl Radiat Isot.* 1982, 33, 1101-1114.

[5] Galante, O. L.; Rodrigues Jr., O.; Campos, L. L. Development of a dosimeter for high doses assessment base don alanine/ EPR. Available from: http://www.irpa.net/irpa10/cdrom/00531.pdf.

[6] Campos, L. L. Termoluminescência de materiais e sua aplicação em dosimetria da radiação. Cerâmica. 1998, 44, 290.

[7] Breen, S. L.; Battista, J. J. Feasibility of reading LiF thermoluminescent dosimeters by electron spin resonance. *Phys Med Biol*. 1999, 44, 8, 2063-9.

[8] Carrilo, R. E.; Pearson, D. W.; Deluca Jr, P. M.; MacKay, J. F.; Lagally, M. G. Response of thermoluminescent lithium fluoride (TLD-100) to photon beams of 275, 400, 500, 600, 730, 900, 1200, 1500, and 2550 eV. *Phys. Med. Biol.* 1994, 39, 1875-1894.

[9] DiMauro, T. Radiochromic Film Dosimetry. Radiation Physics. 2000.

[10] American Society for Testing and Materials. Standard practice for use of a radiochromic film dosimetry system. 2004, ISO/ASTM51275-04, 12.02.

[11] Harwell Dosimeters References . Available from: http://www.harwell-dosimeters.co.uk/references.php

[12] American Society for Testing and Materials. Standard Practice for Use of a Ceric-Cerous Sulfate Dosimetry System. 2002, ISO/ASTM51205-02, 12.02.

[13] American Society for Testing and Materials. Standard Practice for Using the Fricke Reference-Standard Dosimetry System. 2004, E1026-04e1, 12.02.

[14] Harteck, P.; Dondes, S. Nitrous oxide dosimeter for high levels of betas, gammas and thermal neutrons. *Nucleonics*. 1956, 13, 3, 66-72.

[15] Hearne, J. A.; Hummel, R. W. Nitrous as a dosimeter for ionizing radiations. *Radiation Research*. 1961, 15, 254-267.

[16] Harteck, P.; Dondes, S. Radiation chemistry of gases. *Rensselaer Polytechnic Inst*. 1969, 321, 19.

[17] Daros, K. A. C.; Campos, L. L.; Medeiros, R. B. TL response study of the $CaSO_4$:Dy pellets with graphite for dosimetry in beta radiation and low-energy photons fields, *Applied Radiation and Isotopes*. 2001, 54, 6, 957-960.

[18] Optical properties of materials. Available from: http://www.npl.co.uk/optical_radiation/primary_standards/spectrophotometry.html

[19] Spectrophotometry. Available from: http://physics.nist.gov/Divisions/Div844/facilities/specphoto/specphoto.html.

[20] Encyclopedia Britannica online. Electron paramagnetic resonance (EPR). Available from: http://www.britannica.com/eb/article-9032325/electron-paramagnetic-resonance

[21] Bergstrand, E. S.; Shortt, K. R.; Ross, C.K.; Hole, E. O. An investigation of the photon energy dependence of the EPR alanine dosimetry systems. *Phys Med Biol*. 2003, 48, 1753-1771.

[22] Andrew, E. R. Nuclear magnetic resonance, Boston, Cambridge, University Press, 1969.

[23] Advanced undergraduated laboratory. Nuclear Magnetic Resonance. Available from: http://www.physics.utoronto.ca/~phy326/nmr/nmr.pdf.

[24] Stark, D. D.; Bradley, W. G. Magnetic resonance imaging, ed. 2, St. Louis, *Mosby-Tyear Book*, 1992.

[25] Galante, A. M. S.; Rzyski, B. M.; Villavicencio, A. L. C. H.; Campos L. L. The response of potassium nitrate for high-dose radiation dosimetry. *Radiat Phys Chem*. 2002, 63, 719-722

[26] Galante, A. M. S.; Villavicencio, A. L. C. H.; Campos, L. L. Dosimetric properties of KNO_3 pellets mixed with sensitizing compounds. *Radiat Phys Chem*. 2004, 71 (1), 387-389.

[27] Galante, A. M. S.; Villavicencio, A. L. C. H.; Campos, L. L. Preliminary investigations of several new dyed PMMA. *Radiat Phys Chem*. 2004, 71 (1), 393-396.

[28] Galante, A. M. S.; Campos, L. L. Electron dose radiation response of dyed PMMA detectors at IPEN. *Radiat Prot Dos*. 2006, 120, 1-4, 113-116.

[29] Technical Reports Series no. 409. Dosimetry for food irradiation. Printed by the IAEA, Vienna, 2002.

[30] Holm, N. W.; Berry, R. J. Manual on radiation dosimetry. Marcel Dekker, New York, 1970.

[31] Attix, F. H. Introduction to radiological physical and radiation dosimetry. John Wiley & Sons, London, 1986.

[32] Fricke, H.; Hart, E. J. Chemical dosimetry. In: Attix, F. H.; Roesch, W. C. Radiation dosimetry. New York, *Academic*, **3**, 167, 1968.

[33] McLaughlin, W. L.; Boyd, A. W.; McDonald, J. C.; Miller, A. Dosimetry for radiation processing. Taylor & Francis, New York, 1989.

[34] Constantinescu, B. Gamma and proton induced degradation in ceramics material – a Proposal.   Available   from: http://www.iaea.org/programmes/ripc/physics/fec2000/pdf/ftp1_11.pdf

[35] Teixeira M.I.; Ferraz G.M.; Caldas L.V. EPR dosimetry using commercial glasses for high gamma doses. *Appl Radiat Isot*. 2005, 62, 2, 365-70.

[36] Caldas, L. V. E.; Teixeira, M. I. Comercial glass for high doses using different dosimetric techniques. *Radiat Protec Dosim*. 2002, 101, 1-4, 149-152.

[37] Hsu, S. M.; Yeh, S. H.; Lin, M. S. and Chen, W. L. Comparison on characteristics of radiophotoluminescent glass dosemeters and thermoluminescent dosemeters. *Radiat Prote Dosim*. 2006, 119, 1-4, 327-331.

[38] Semiconductor   detector.   Available   from: http://www.radiofreeithaca.net/search/Semiconductor_detector

[39] Rasolonjatovo, A. H. D.; Shiomi, T.; Nakamura, T. Development of gamma-ray monitor using   CdZnTe   semiconductor   detector.   Available   from: http://www.irpa.net/irpa10/cdrom/00110.pdf

[40] Patil, S. F.; Chiplunkar, N. R. Influence of oxides on the radiolysis of $RbNO_3$ e $CsNO_3$. *Radiat Phys Chem*. 1991, 37, 2, 241-244.

[41] Joshi, N. G.; Garg, A. N.; Natarajan, V.; Sastry, M. Effect of oxide additives on radiolytic decomposition of zirconium and thorium nitrates. *Radiation Measurements*. 1996, 26, 1, 131-137.

[42] Pogge, H. B.; Jones F. T. The effect of temperature and additives in the radiolysis of potassium nitrate. *J Phys Chem*. 1970, 74, 8, 1700-1705.

[43] Parwate, D. V.; Garg A. N. Effect of outer cations and water of crystallization on the radiolytic decomposition of nitrates. *J Radioanal Nucl Chem Lett*. 1984, 85, 4, 203-212.

[44] Patil, S. F.; Bedekar, A. G. Radiation decomposition of pure and barium doped potassium nitrate and effect of oxides thereon. *Radiochimica Acta*. 1985, 38, 165-168.

[45] Kulkarni, S. P.; Garg, A. N. Effect of additives with common cation on the radiolysis of ammonium, sodium and potassium nitrates in admixtures. *Radiat Phys Chem*. 1988, 32, 4, 609-614.

[46] Batra, R. J.; Garg, A. N. Gamma radiolytic decomposition of solid binary mixtures of potassium nitrate with halide. *J Radioanal Nucl Chem Art*. 1989, 129, 1, 155-162.

[47] Joshi, N. G.; Dhoble, S. J.; Moharil, S. V.; Garg, A. N. Effect of particle size on gamma ray induced decomposition in KI-KNO$_3$ crystals. *Radiat Phys Chem*. 1994, 44, 3, 317-322.

[48] Agrawal, N.; Garg, A. N. Effects of oxide additives on radiolytic decomposition of potassium nitrate. In: TSRP-98 Trombay. Symposium on Radiation and Photochemistry. Mumbai, India, 1999.

[49] American Society for Testing and Materials. 1996. Standard practice for use of a polymethylmethacrylate dosimetry system, (ASTM E 1276 – 96), Annual Book, 12.02.

[50] Bero, M. A.; Gilboy W. B. and Glover P. M. Radiochromic gel dosemeter for three-dimensional dosimetry. *Radiat Phys Chem*. 2001, 61, 433-435.

[51] Bero M. A. and Kharita M. H. Effects of ambient temperature on the FXG radiochromic gels used for 3-D dosimetry. *Journal of Physics*: Conference Series 3, 2004, 213-216.

[52] Bero M. A.; Gilboy W. B. High-resolution optical tomography for 3-D radiation dosimetry with radiochromic gels. *Journal of Physics*: Conference Series 3, 2004, 261-264.

[53] Gore J. C.; Kang Y. S.; Shulz, R. J. Measurement of radiation dose distributions by nuclear magnetic resonance (NMR) imaging. *Phys Med Biol*. 1984, 29, 10, 1189-1197.

[54] Healy, B.; Brindha S.; Zahmatkesh M.; Baldock, C. Characterization of the ferrous-xylenol orange-gelatin (FXG) gel dosimeter. *Journal of Physics*, Conference Series 3, 2004, 142-145.

[55] Jayachandran C. A. Calculated effective atomic number and kerma values for tissue-equivalent and dosimetry materials". *Phys Med Biol*. 1971, 16, 4, 617-623.

[56] Olsson L. E.; Appleby A.; Sommer, J. A new Dosimeter Based on Ferrous Sulphate Solution and Agarose Gel. *Appl Radiat* Isot. 1991, 42, 11, 1081-1086.

[57] Schulz R. J.; DeGuzman A. F.; Nguyen D. B.; Gore J. C. Dose-Response Curves for Fricke-Infused Agarose Gels as Obtained by Nuclear Magnetic Resonance. *Phys Med Biol*. 1990, 35, 12, 1611-1622.

[58] Dorda, E. M.; Muñoz, S. S. Potassium Nitrate/ Nitrite Dosimeter for high-dose. In: High-dose dosimetry, Proceeding of an International Symposium. 1984, IAEA SM 272/1, Vienna.

[59] Torres C., R. R. Medición de altas dosis de radiación gamma por el sistema nitrate-nitrito de potasio. Callao, Peru. 1993, Tese, Universidade del Callao.